Fast Online Parameter Identification for Current Source Operated PV Modules in DC Microgrids

AHMED M. A. OTEAFY[iD], **(Senior Member, IEEE),**
ABDULRAHMAN ABOMAZID[iD], **(Member, IEEE),**
AND ARAM S. MONAWAR, (Member, IEEE)
Joint Smart Grids and Electric Vehicles Research and Development Center (JSEC), Alfaisal University, Riyadh 11533, Saudi Arabia

Corresponding author: Ahmed M. A. Oteafy (aoteafy@alfaisal.edu)

ABSTRACT This paper presents a non-iterative online approach to identify the modeling parameters of a photovoltaic (PV) module. It is motivated by the fact that accurate and reliable modeling of distributed energy resources (DERs) in DC Microgrids improves their stability and efficiency under a wide range of operational conditions. In particular, the case where PV modules are used as DERs in their current-source region is considered. The proposed method addresses the limitations associated with parameter identification in these settings. Specifically, the method works under varying temperature and insolation conditions relying only on current and voltage sensors that already exist in the power electronic converters tying the PV DER to the Microgrid. Also, its algorithm is practical and reliable as it does not rely on *a priori* knowledge or an initial guess, and it is non-iterative, so it does not risk divergence (or require proof of convergence) as other iterative algorithms. Moreover, it is both fast and of a low computational complexity, which enables its implementation on microcontrollers within PV DER systems. The development of this method is detailed in the paper along with its application steps to facilitate its adoption. Furthermore, an experimental setup was used to test the proposed method under different ambient conditions and demonstrated its efficacy with algorithm execution times of under 1 second and high modeling accuracy on a microcontroller.

INDEX TERMS Photovoltaic system modeling, DC microgrids, parameter identification, maximum power point, non-iterative techniques.

NOMENCLATURE

PV MODEL VARIABLES AND PARAMETERS

N_s	Number of cells in series forming a string.
N_p	Number of strings in parallel in a module.
V_c, I_c	Cell terminal voltage and current.
V	Module terminal voltage, $=N_s V_c$.
I	Module terminal current, $=N_p I_c$.
P_m	Module maximum power point (MPP).
V_m, I_m	Module voltage and current at MPP.
I_{ph}	Cell photoelectric current.
I_d	p-n junction diode current.
I_0	p-n junction diode scaling (saturation) current.
V_T	p-n junction thermal voltage.
S	Module insolation.
T	p-n junction Temperature.
n	p-n junction ideality factor.

α	scaling factor, $=nV_T$.
R_s	Cell series resistance.
R_p	Cell parallel (shading) resistance.
G_p	Cell parallel conductance, $=1/R_p$.

PV MODELS

SDM	Single diode model.
SSDM	Simplified SDM, eliminates R_s.
ISDM	Ideal SDM, eliminates R_s and R_p.

IDENTIFICATION MODEL

y, W	Regressor vector and matrix.
K	Vector of unknown parameters.
N	Total number of sampled data points.
n	Index of sampled data points.
EI	Identification model error index.
RE	Relative error at a key operating point.
$\bar{e}_x$	Normalized relative error of a variable x.

The associate editor coordinating the review of this manuscript and approving it for publication was Amin Hajizadeh.

I. INTRODUCTION

Photovoltaic (PV) systems are becoming the main distributed energy resource (DER) of choice in modern-day deployment of renewables. Whether these PV systems are on rooftops or part of a large-scale power plant, they are competitively bringing down the cost of renewables in the electric power production market. In medium to large-scale PV systems, PV modules are connected in strings with a string inverter converting their DC power to an AC bus supplying power to the main grid. PV DER modules can alternatively be connected within an autonomous Microgrid. Modeling their performance in these Microgrids is essential for their reliable operation.

A. PV SYSTEMS IN DC MICROGRIDS

Relatively recent paradigms consider integrating PV systems within DC microgrids; see the surveys by Olivares *et al.* [1], Dragicevic *et al.* [2], and Chen *et al.* [3]. These Microgrids are electrical networks consisting of DERs, loads, Energy Storage Systems (ESS's), and supervisory control and data acquisition (SCADA) systems. They allow an entity, e.g., a university campus or a neighborhood, to have autonomous operation that can be either *islanded* from or *connected* to the main AC power grid. Optimal operation of these Microgrids requires modeling of their modules to achieve and maintain their autonomous, resilient, and maximum power production capabilities. Therefore, effective models of PV modules that are both accurate and practically identifiable are needed to overcome difficulties in active control, failure detection, Maximum Power Point (MPP) identification and tracking, and overall reliable operation of the DERs within Microgrids. This is particularly important when insolation and temperature conditions change throughout the day. Accurate current vs. voltage *I-V* and power vs. voltage *P-V* models are also required to deliver specific power outputs and achieve balanced operation. Moreover, PV systems can be operated in their current-source or voltage-source regions. Either region along with the MPP can be sufficient in providing the full range of operating points (and power outputs) for the DC Microgrid. The current-source region is suitable when the Microgrid is of a low voltage or an isolated high-frequency DC to DC converter is used, while the voltage-source region is especially suited to more efficiently achieve a high step up in DC voltage when a non-isolated boost converter is used.

B. PV CIRCUIT MODELS

Researchers have considered several lumped-parameter circuit models of a PV cell in order to obtain its characteristic *I-V* and *P-V* curves. Moreover, they, e.g., Kennerud [4] and Masters [5], have detailed the impact of parameter variations within these models on the characteristic curves and the performance of the PV cell. The models directly extend to panels with cells connected in series to form a string providing more voltage as well as strings connected in parallel providing more current. Furthermore, the model can be extended for panels connected to form an array. The simplest model of the PV cell includes an insolation dependent current-source in parallel with a diode representing its p-n junction. This model, known as the Ideal Single-Diode Model (ISDM), captures the nonlinear *I-V* relationship under varying temperature and insolation conditions. Three parameters are key to this model, namely, a photoelectric current I_{ph}, a diode scaling current I_0, and an exponential term scaling factor α itself the product of the diode's ideality factor n and thermal voltage V_T. However, the ISDM cannot explain the existence of a parallel resistive path within the cell that is especially important for modeling partially shaded panels, and it does not explain the voltage regulation effects occurring near the open-circuit condition due to the effective series resistance of the path to the terminals of the cell [5]. Therefore, a more accurate model adds a parallel resistance R_p and a series resistance R_s to model these two phenomena, respectively. This results in a five parameter nonlinear Single-Diode Model (SDM). Other higher precision models exist for the PV cell that include a double-diode model [6], [7] or even a triple-diode model [8]. However, the parameter identification for such models is more complex and requires *a priori* data due to their high degree of nonlinearity. A commonly proposed simplification of the SDM is to eliminate R_p. Instead, we propose to eliminate R_s referring to this model as the Simplified SDM, or SSDM.

C. PARAMETER IDENTIFICATION

A parameter identification method is then required to fit the model of a given PV module. In the literature, the majority of these methods rely on data collected over the full range of the *I-V* curve from the short-circuit current I_{sc} to the open-circuit voltage V_{oc} operating points to fit the SDM. Kennerud [4], for example, used specific points on the *I-V* curve including the slopes near I_{sc} and V_{oc} in an iterative algorithm to simultaneously solve a set of nonlinear equations for the parameters. He demonstrated the impact of varying each parameter on the performance of the PV cell. Similarly, Haouari-Merbah *et al.* [6] employed an iterative technique to identify the parameters of the SDM model. They emphasized the importance of avoiding measurement errors in current and slope calculations near the V_{oc}, and those in the voltage near the I_{sc}. Also, Phang *et al.* [9] used the same points as [4] including the *I-V* curve slopes in addition to the junction temperature measurement, but they solve for the parameters directly in a non-iterative manner with some simplifications. Toledo *et al.* [10] have utilized a linear least-squares method to find the parameters of the SDM in a non-iterative manner as a first step. This generates a large but finite number of parameter sets that are then searched for the set that yields the minimum error between the estimated curve and the data. Next, the authors use a refinement process to further reduce the modeling error in the identified parameter set. This method is both non-iterative and precise, however, the search step and refinement processes can limit its use in online parameter identification. Moshksar and Ghanbari [11]

reduce the model equations by reformulating them in terms of the independent variables, and then solving the resulting set of equations as a convex optimization problem, without *a priori* information, using an adaptive gradient descent iterative method. Lim *et al.* [12] use a different *linear* approach, where the nonlinear SDM is converted into the problem of solving a set of linear differential equations, using the Laplace transform, to obtain the parameters. However, the value of R_s must be iteratively adjusted in an outer loop containing the integrals of the differential equations until the algorithm converges.

Alternatively, using information from the data sheet of the PV panel, the SDM model parameters were identified using iterative algorithms by Sera *et al.* [13] and by Villalva *et al.* [14]. In both these cases, the model accounts for variations in temperature and insolation, which facilitates using them in circuit simulation models. If instead both R_s and R_p are ignored, the simpler ISDM can be solved explicitly as shown by [15] but this results in a lower modeling accuracy.

On the other hand, *linear* polynomial curve fitting of the SDM model was used by several researchers, see Xiao *et al.* [16], Andrei *et al.* [17], Paviet-Salomon *et al.* [18] and references therein. This approach results in polynomials of orders ranging from four to eight (depending on the type of PV cell and the number of data points extracted from the *I-V* curve), which simplifies solving for specific operating points instead of iteratively solving the nonlinear PV models. A comparison was performed by Ibrahim and Anani [19] between different methods. It showed that some analytical techniques with simplified models can produce comparable results to iterative methods of higher computational cost.

Moreover, a wealth of heuristic and meta-heuristic algorithms have been developed for the parameter identification of PV modules. Genetic Algorithms (GA) and Particle Swarm Optimization (PSO), for example, were utilized in [20], [21] to identify the parameters of PV cells. A PSO is employed in [22], which involves a large amount of input data to the algorithm in order to extract the cell parameters. For the double diode model (DDM), Bradaschia *et al.* [23] use a combination of analytical equations and a pattern search iterative algorithm to estimate them. An improved multiswarm PSO iterative algorithm was developed by Nunes *et al.* [24] for the DDM that achieves high modeling accuracy, and it takes about a minute for convergence on a 3.6 GHz CPU. In [25], a modified flower pollination algorithm (FPA) is presented to estimate the parameters of SDM and DDM of PV cells and modules. Despite its accuracy, the algorithm requires a high number of iterations before it converges. Using an improved opposition-based tunicate swarm algorithm (OTSA), the work in [26] estimates the parameters of SDM for polycrystalline and monocrystalline PV modules. For PV SDM and DDM modules, a chaotic gradient-based optimization (CGBO) algorithm is proposed in [27] to find their parameters. In [28], a dynamic self-adaptive and mutual-comparison teaching-learning-based optimization (DMTLBO) algorithm is presented for

TABLE 1. Summary of parameter identification methods.

PV Models	Parameter Identification Methods
ISDM	Non-iterative explicit solution [15].
SDM	Iterative [4], [6], [11]–[14]; iterative for online operation [30]; non-iterative requiring more information & simplifications [9]; non-iterative but suited for offline operation [10]; iterative heuristic methods using GA [20] and PSO [21], and iterative meta-heuristic methods using enhanced FPA [25], improved OTSA [26], CGBO [27], and DMTLBO [28].
Polynomial	Polynomials with orders that vary depending on cell type, region of interest, convergence, desired accuracy, and other factors [16]–[18].
DDM	Heuristic methods including iterative pattern search [23], improved multiswarm PSO iterative algorithm [24]; and iterative meta-heuristic methods using enhanced FPA [25], CGBO [27], DMTLBO [28], and improved learning search algorithm [29].

extracting PV parameters. Also, Huang *et al.* [29] developed a meta-heuristic search algorithm for the SDM and DDM models that is self-adaptive in the iteration steps. The results of their algorithm are precise, however, it takes minutes to conclude on a CPU. Such algorithms have a high computational complexity and are therefore suited for offline parameter identification.

Therefore, depending on the application at hand, the PV system requires a specific model coupled with an effective parameter identification method. The aforementioned techniques are more than adequate to address applications such as offline characterization (e.g., for certification) or the development of simulation models, however, they are not practical for online identification. More recently, online parameter identification was addressed by Lappalainen *et al.* [30] for the SDM model using the data sheet information as an initial guess, with an iterative technique that modifies the parameter values to best fit the measured *I-V* curves.

The aforementioned literature on parameter identification methods can be summarized as shown in Table 1.

In this work, an online parameter identification method is developed and demonstrated that is capable of:

1) Accurately identifying the MPP.
2) Identifying any specific output power operating point.
3) Operating under varying insolation and temperature.
4) Online parameter identification, i.e., conducted while the PV system is supplying power to a DC Microgrid.
5) Using a limited data range, without pre-identification of I_{sc}, V_{oc}, the MPP, or any other operating point.
6) Fast operation with minimal memory complexity when implemented on a microcontroller.
7) Reliable determination of SSDM model parameters.

As such, to the best knowledge of the authors, it is the only online identification method that is non-iterative and accurately models the PV module in the current-source region of operation. Reliability of iterative techniques requires proof of convergence, otherwise they can risk diverging during
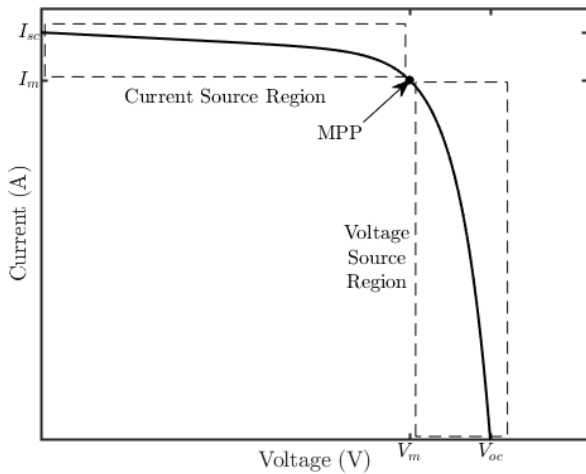
FIGURE 1. Typical PV module *I-V* curve and its regions of operation.
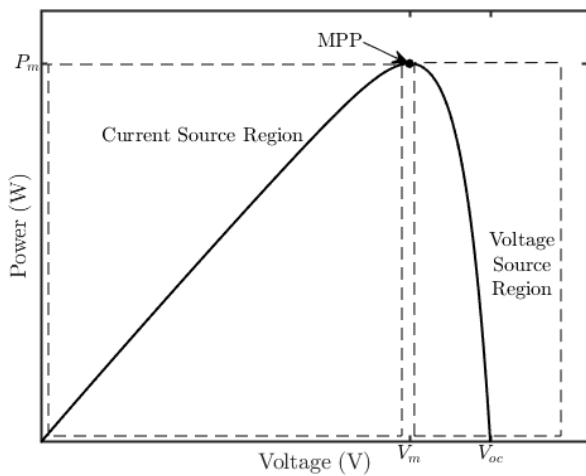
FIGURE 2. Typical PV module *P-V* curve and its regions of operation.

FIGURE 3. PV cells circuit diagrams (a) Ideal Single-Diode Model (ISDM) (b) Single-Diode Model (SDM) (c) Simplified Single-Diode Model (SSDM).

online operation. The remainder of the paper is organized as follows: The proposed PV cell and module models are given in Section II. In Section III, the equations underlying the proposed parameter identification method are developed. This is followed by an experimental validation of the proposed method and an outline of its practical implementation in Section IV. Conclusions are drawn in Section V with suggestions for future work.

II. PROPOSED PV MODELING
The modeling of any DER, and indeed any electrical device, starts with obtaining its *I-V* characteristic curve at its terminals. As a DER the power output capability at different voltage levels is also important, and is represented by its *P-V* characteristic curve. For a PV module, the *I-V* and *P-V* curves depicted in Figures 1 and 2, respectively, represent a typical PV module and can be obtained offline by varying a connected resistive load between the short-circuit and open-circuit operating points, registering I_{sc} and V_{oc}, respectively.

Moreover, when a PV DER is connected to a Microgrid through a power electronic converter, several operating modes are possible. It can regulate its duty ratio to attain the MPP, noting that V_m and I_m are the voltage and current at the MPP, and P_m is the MPP. Alternatively, it can target an operating point with a specific lower power output (to balance the Microgrid) either in the current-source region or in the voltage-source region. The type of converter used depends on the voltage level at the main bus of the Microgrid. So, for example, if a higher level DC voltage is required at the main bus, a boost converter is used, and in practice, if the current-source region is selected, the exact short-circuit condition and its neighboring region is not reachable due to the voltage drop across the power transistor used by the boost converter. This fact can limit the amount of data collected by an online parameter identification method. Also, operating online in one region (e.g., the current-source) may limit the amount of data collected in the other (e.g., voltage-source). So online parameter identification techniques must account for limitations in data collection.

A. PV CELL MODEL
As previously mentioned, the simplest model to consider for a PV cell is the ISDM in Figure 3a, which consists of a current-source generated by insolation and is connected in parallel to a p-n junction diode model of the cell. Accounting for the linear drop in the output current in the current-source region requires R_p, and similarly, the voltage regulation effect in the voltage-source region requires R_s. Including both these resistances in the circuit model results in the SDM shown in Figure 3b. In this work, we focus on the operation of the PV system as a DER tied to a DC Microgrid in the current-source region, including the MPP. Therefore, we propose using a simplified SDM (SSDM) eliminating R_s as shown in Figure 3c, and keeping R_p, which is the basis for developing a practical real-time online approach in this work. However, for other applications where voltage-source operation is desired, either the SDM or a simplified SDM that only ignores R_p should be used.
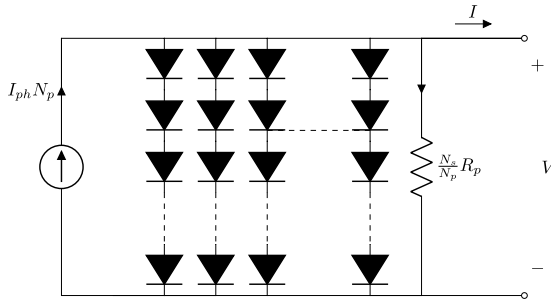
FIGURE 4. Proposed PV module circuit model.

The resulting PV cell model is given by the I-V relationship:

$$I_c = I_{ph} - I_d - I_p = I_{ph} - I_0[e^{\frac{V_c}{nV_T}} - 1] - \frac{V_c}{R_p}, \quad (1)$$

where I_c is the cell output current, I_{ph} is the photoelectric current that is proportional to the insolation, I_d is the p-n junction diode recombination current, I_p is the current in the parallel path through the cell, I_0 is the scaling current, V_c is the cell terminal (output) voltage, n is the ideality factor of the p-n junction, and V_T is the thermal voltage.

Given that R_s is ignored in this model, the terminal voltage V_c is equal to the voltage appearing across the p-n junction. Also, under short-circuit conditions $I_{sc} = I_{ph}$.

Defining a scaling factor $\alpha = nV_T$, accounts for variations in n for different types of PV cells (different p-n junction electron-hole recombination processes) and in V_T that varies with temperature as $V_T = kT_c/q$, where k is Boltzmann's constant (1.3806×10^{-23} J/K), T_c is the p-n junction temperature, and q is the electron charge (1.6021×10^{-19} C).

Accordingly, the PV cell model is given by

$$I_c = I_{ph} - I_0[e^{\frac{V_c}{\alpha}} - 1] - \frac{V_c}{R_p}. \quad (2)$$

Finally, during the operation of the PV cell, $I_{ph} \gg I_0$, therefore, the model simplifies to

$$I_c = I_{ph} - I_0 e^{\frac{V_c}{\alpha}} - \frac{V_c}{R_p}, \quad (3)$$

with four model parameters to be identified at any given temperature and insolation level, namely, I_{ph}, I_0, α and R_p.

B. PV MODULE MODEL
The proposed SSDM can be extended to a module with N_s cells connected in series forming a string, and N_p strings in parallel forming a module. Its circuit is depicted in Figure 4. Then, the terminal voltage and current are related to the cell voltage and current by $V = N_s V_c$ and $I = N_p I_c$, respectively.

The I-V characteristics for the PV module are therefore

$$I = N_p I_c = N_p I_{ph} - N_p I_0 e^{\frac{V_c}{\alpha}} - \frac{N_p V_c}{R_p}. \quad (4)$$

Substituting for $V_c = V/N_s$ we have

$$I = N_p I_{ph} - N_p I_0 e^{\frac{V}{N_s \alpha}} - \frac{N_p V}{N_s R_p}. \quad (5)$$

Then, in application, the PV module model in (5) may be used or, alternatively, a scaled model that has the same form as (3) but represents the *average* performance of the cells in the module, that is,

$$I_c = I_{ph} - I_0 e^{\frac{V_c}{\alpha}} - \frac{V_c}{R_p}. \quad (6)$$

To use this scaled model, the measured V and I are simply divided by N_s and N_p to obtain the scaled voltage V_c and current I_c, respectively. Note that this scaled model is not the actual performance of any individual cell due to mismatches, e.g., in the fabrication of the cells.

III. PARAMETER IDENTIFICATION MODEL DERIVATIONS
Using the scaled PV module model (6), two sets of identification model equations can be derived to obtain the unknown parameters. The process is non-iterative and uses data collected over a limited range of the I-V curve. The known parameters are the number of cells in series N_s and the number of strings in parallel N_p. The measurable variables are I and V of the PV module, from which the scaled variables $V_c = V/N_s$ and $I_c = I/N_p$ are directly computed. These variables are measured in a range starting near the short-circuit condition up to any point beyond the MPP, i.e., towards the open-circuit condition. The N recorded data points are arranged with an index of $n = 1, 2, \ldots, N$. The unknown parameters to be found are the parallel resistance per cell R_p, the photoelectric current I_{ph}, the scaling factor α, and the scaling current of the p-n junction model I_0. Note that any variations in junction temperature and insolation are captured by identifying these parameters, so only current and voltage sensors are required for data collection.

A. IDENTIFICATION OF I_{ph} AND R_p
The first identification model is used to find I_{ph} and R_p. Near the short-circuit operating point $V_c \approx 0$, and (6) simplifies to

$$I_c \approx I_{ph} - G_p V_c, \quad (7)$$

where, the parallel conductance $G_p = 1/R_p$. This can be written in regressor form as

$$y = WK, \quad (8)$$

where,

$$y \triangleq I_c, \quad W \triangleq [1 \quad -V_c], \quad K \triangleq [\kappa_1 \quad \kappa_2]^T \triangleq [I_{ph} \quad G_p]^T.$$

That is, y and W are known from the measured variables, and K contains the unknown parameters. To solve this regressor, N_{sc} data points that are sampled near the short-circuit operating point are used. These samples are indexed as

$n = 1, 2, \ldots, N_{sc}$. To find the vector K, we define the mean squared error as

$$E^2(K) = \sum_{n=1}^{N_{sc}} (y(n) - W(n)K)^2. \tag{9}$$

Multiplying out we get

$$E^2(K) = R_y - R_{Wy}^T K - K^T R_{Wy} + K^T R_W K, \tag{10}$$

where,

$$R_y = \sum_{n=1}^{N_{sc}} y^2(n),$$

$$R_W = \sum_{n=1}^{N_{sc}} W^T(n)W(n),$$

$$R_{Wy} = \sum_{n=1}^{N_{sc}} W^T(n)y(n). \tag{11}$$

If the data collected sufficiently excites the model then R_W will be invertible, and we can minimize the error by

$$\frac{\partial E^2(K)}{\partial K} = -2R_{Wy} + 2R_W K = 0, \tag{12}$$

or

$$K = R_W^{-1} R_{Wy}. \tag{13}$$

Note that $V_c(n)$ is nonnegative over the range of $n = 1, \ldots, N_{sc}$, with one zero value at the short-circuit operating point and positive values otherwise. Therefore, the matrix $W^T(n)W(n)$ is full rank and so is R_W. Consequently, R_W is invertible and (13) will yield $\kappa_1 = I_{ph}$ and $\kappa_2 = G_p$ where $R_p = 1/G_p$, which minimize the squared error in (10). Notwithstanding the fact that R_W is full rank, it is important to use Gaussian elimination or LU decomposition to obtain R_W^{-1} in real-time implementation, as opposed to calculating it through the adjugate matrix. This minimizes numerical errors and is common practice in linear algebra libraries such as the `BasicLinearAlgebra` library [31] used on the Arm Cortex M3 microcontroller in this work.

B. IDENTIFICATION OF α AND I_0

This step is used to identify the scaling factor α of the exponential term and the scaling current I_0. Differentiating I_c with respect to V_c, i.e., for any two neighboring points on the I-V curve

$$\frac{\partial I_c}{\partial V_c} = -\frac{1}{\alpha} I_0 e^{\frac{V_c}{\alpha}} - \frac{1}{R_p}, \tag{14}$$

or

$$\alpha \frac{\partial I_c}{\partial V_c} + \alpha \frac{1}{R_p} = -I_0 e^{\frac{V_c}{\alpha}}. \tag{15}$$

Substituting back in (6) and rearranging gives

$$I_{ph} - I_c - \frac{V_c}{R_p} = \alpha \left(-\frac{\partial I_c}{\partial V_c} - \frac{1}{R_p} \right). \tag{16}$$

Note that in normal operation, the left hand side of (16) is always positive, and the derivative $\partial I_c / \partial V_c$ is always negative. Next, rearranging (6)

$$I_{ph} - I_c - \frac{V_c}{R_p} = I_0 e^{\frac{V_c}{\alpha}}. \tag{17}$$

Now, taking the natural logarithm of both sides, which are always nonnegative, and rearranging we obtain

$$V_c = \alpha \ln \left(I_{ph} - I_c - \frac{V_c}{R_p} \right) - \alpha \ln(I_0). \tag{18}$$

Combining (16) and (18) in regressor form we get

$$y_2 = W_2 K_2, \tag{19}$$

where,

$$y_2 \triangleq \left[I_{ph} - I_c - \frac{V_c}{R_p} \quad V_c \right]^T,$$

$$W_2 \triangleq \begin{bmatrix} -\dfrac{\partial I_c}{\partial V_c} - \dfrac{1}{R_p} & 0 \\ \ln \left(I_{ph} - I_c - \dfrac{V_c}{R_p} \right) & 1 \end{bmatrix},$$

$$K_2 \triangleq \begin{bmatrix} \kappa_3 & \kappa_4 \end{bmatrix}^T \triangleq \begin{bmatrix} \alpha & -\alpha \ln(I_0) \end{bmatrix}^T.$$

As with the previous regressor, y_2 and W_2 are known from the measured variables, and K_2 is the unknown parameter. In this case, however, the data points $n = N_{sc}, N_{sc} + 1, \ldots, N$ are used to avoid singularity in the matrix W_2 near the short-circuit condition, as $\partial I_c / \partial V_c \approx -1/R_p$, resulting in a zero row. Therefore, with this selected data range, singularity can be avoided in the matrix W_2 and consequently in R_{W2}. The squared error is calculated as

$$E^2(K_2) = R_{y2} - 2R_{Wy2}^T K_2 + K_2^T R_{W2} K_2, \tag{20}$$

where,

$$R_{y2} = \sum_{n=N_{sc}}^{N} y_2^T(n)y_2(n),$$

$$R_{W2} = \sum_{n=N_{sc}}^{N} W_2^T(n)W_2(n),$$

$$R_{Wy2} = \sum_{n=N_{sc}}^{N} W_2^T(n)y_2(n). \tag{21}$$

Then, K_2 can be found as

$$K_2 = R_{W2}^{-1} R_{Wy2}, \tag{22}$$

minimizing the squared error in (20), with the remaining SSDM PV model parameters $\alpha = \kappa_3$ and $I_0 = \exp(-\kappa_4/\kappa_3)$.

IV. IMPLEMENTATION AND RESULTS

The proposed PV parameter identification approach is demonstrated experimentally in this section. First, validation metrics are defined, and then, the implementation procedure is outlined to clarify and facilitate its practical application. Next, the experimental setup is described, and the results are detailed to discuss the effectiveness of the proposed method using a microcontroller to perform the measurements and calculations.

A. VALIDATION METRICS

The accuracy of the parameter identification method is validated using three different metrics: an Error Index for each identification model equation, the relative errors at the MPP operating points, and a normalized relative error over the current-source and voltage-source ranges.

The error index relates to the squared error in (10) and (20). It determines whether the identified parameters provide a good fit for the data, see [32]–[34], and is defined as

$$EI \triangleq \sqrt{\frac{E^2(K^*)}{E^2(0)}} = \sqrt{\frac{R_y - 2R_{wy}^T K^* + K^{*T} R_W K^*}{R_y}} \leq 1. \tag{23}$$

where the squared error is evaluated with the estimated parameter vector $K = K^*$ and compared to the squared error if we arbitrarily select zeros as the estimated parameters. The result should be less than one; otherwise the estimated value is as good as any arbitrary set of parameters. Two error indices with subscripts 1 and 2, are used for identification model equations (13) and (22), respectively.

Also, the MPP is a key operating point, and a relative error can be calculated as

$$RE = \left| \frac{x_{exp} - x_{est}}{x_{exp}} \right| \times 100\%, \tag{24}$$

where, x_{exp} represents the V_m, I_m, and P_m obtained from the measured data, and x_{est} represents their estimated counterparts from the SSDM after the proposed parameter identification is conducted.

Additionally, the normalized relative error (NRE) between the collected *I-V* data and the estimated model curve can be directly calculated [33], [35], and is defined as follows

$$\bar{e}_x \triangleq \frac{1}{N_2 - N_1} \sum_{n=N_1}^{N_2} \left| \frac{x_{act}(nT) - x_{est}(nT)}{x_{act}(nT)} \right|, \tag{25}$$

where, x is the state variable of interest, x_{est} is its estimated counterpart, and N_1 and N_2 are the start and end data points. Specifically, two NRE values calculated, namely, $\bar{e}_I$ and $\bar{e}_V$ corresponding to the current-source and voltage-source regions, respectively. For $\bar{e}_I$, data collection starts near the short-circuit condition at $N_1 = 1$ up to $N_2 = N_{MPP}$, while for $\bar{e}_V$, the voltage-source region starts at $N_1 = N_{MPP}$ up to $N_2 = N$. That is, the MPP is included in both NRE calculations.
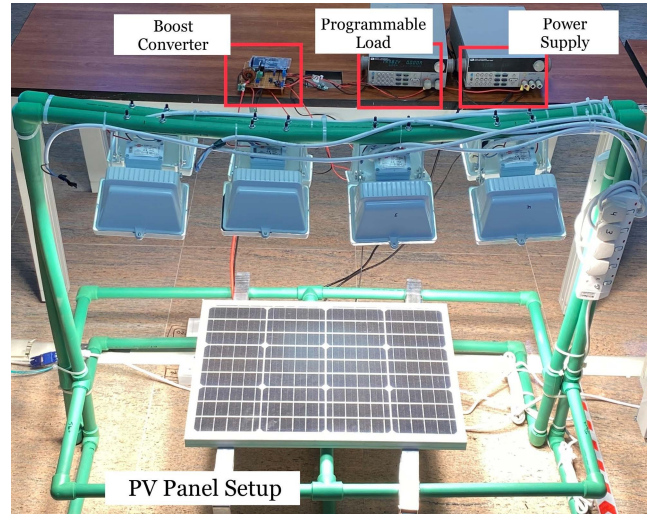
FIGURE 5. Experiment setup.

B. PARAMETER IDENTIFICATION STEPS

The online implementation of the parameter identification method is summarized as follows:

1) Collect $I[n]$ and $V[n]$ for data points $n = 1$ to N. E.g., vary the duty ratio D of the boost converter over its online operational range $D \in [D_{min}, D_{max}]$ in increments $D_{inc} = (D_{max} - D_{min})/N$.
2) Apply a low pass filter on the data, to remove the impact of the boost converter PWM and measurement noise.
3) Determine the range of filtered data $n = 1$ to $n = N_{sc}$ near the short-circuit operating point, e.g., all data points from $I[1]$ down to 90% of $I[1]$, i.e., $I[N_{sc}] \approx 0.90 \, I[1]$.
4) Use this data to calculate R_y, R_{Wy} and R_W in (10). Then, find the parameters I_{ph} and R_p using (13), and compute EI_1 to check that it is less than 1, see (23).
5) Use the range of of filtered data $n = N_{sc}$ to N for the second identification model by first calculating the partial derivative $\partial I_c / \partial V_c$ using the center difference approach at every n.
6) Then, use them along with the estimated I_{ph} and R_p to calculate R_{y2}, R_{Wy2} and R_{W2} in (20) to find the parameters α and I_0 using (22) and compute EI_2.

The parameter identification algorithm can be implemented online in a DC Microgrid for any PV DER module as often as is necessary to keep track of changing temperature and insolation conditions. Moreover, changes in the parameters beyond a certain range, e.g., in R_p, can be used to detect the end-of-life or degradation in the PV module.

C. EXPERIMENT: DC MICROGRID CONNECTED PV MODULE

The experimental setup represents a PV DER connected to the regulated bus of a DC Microgrid through a power electronic converter. It consists of a PV module, eight halogen lamps, a boost converter controlled by an Arm Cortex
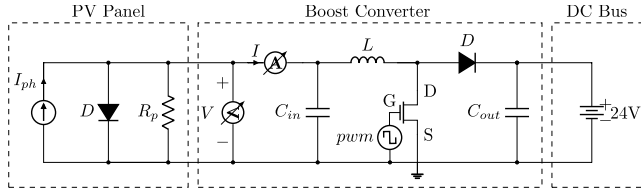
FIGURE 6. Equivalent circuit diagram of the experimental setup.

M3 microcontroller in an Arduino Due board, and a programmable DC voltage load. The setup is shown in Figure 5, and its equivalent circuit diagram is depicted in Figure 6. Specifically, the boost converter has an input capacitance $C_{in} = 47\ \mu F$, an output capacitance $C_{out} = 470\ \mu F$, and an inductance $L = 250\ \mu H$. Note that the conditions of a DC microgrid bus were created by setting the programmable load to constant voltage load mode with $V_{bus} = 24\ V_{dc}$, and using an external 12 V_{dc} supply to consistently power the microcontroller and its sensing circuit. The halogen lamps are a cost-effective replacement for actual solar irradiance in a lab setup, but are not identical to it. Specifically, there is a higher proportion of photons in the infrared and red range of the irradiance spectrum. Therefore, if the objective of the setup is, for example, the certification of PV panels under standard testing conditions (STC), halogen and LEDs can be combined to construct a hybrid lamp as discussed in [36] for a class A solar simulator. However, in this setup only halogen lamps were used. Moreover, to create different insolation levels, layers of sunshade film are placed directly on the PV panel, and to create different PV panel temperature conditions two variable speed fans are placed at opposite sides of the setup. A USST50-36M monocrystalline PV panel is used, which provides 50 watts maximum power at STC. Table 2 shows the electrical characteristics and specifications of the solar panel. The sensors used were a voltage and current sensor at the input (PV Panel) side of the converter and a digital temperature sensor (DS18B20) that was placed below the panel to record the junction temperature (not needed by the algorithm). Moreover, the insolation was calculated using the direct proportionality relationship between I_{sc} and S, that is, the estimated $I_{sc} = I_{ph}$ in the SSDM is used to get an approximate value for the insolation (as I_{sc} slightly increases with temperature) as follows

$$S \approx \frac{S_{STC}\, I_{sc}}{I_{sc,STC}}. \qquad (26)$$

TABLE 2. Electrical characteristics of the USST50-36M PV module.

Maximum power at STC ($P_{m,STC}$)	50 W
Optimum Operating Voltage ($V_{m,STC}$)	18.1 V
Optimum Operating Current ($I_{m,STC}$)	2.76 A
Open-Circuit Voltage ($V_{oc,STC}$)	22.1 V
Short-Circuit Current ($I_{sc,STC}$)	2.93 A

The proposed parameter identification algorithm was implemented on the microcontroller by first varying the duty ratio of the boost converter from 0% to 99% and collecting $N = 1000$, I and V data points. The PWM frequency was set to $f_{PWM} = 64kHz$ with a controller time of $T_{con} = 0.5ms$ between duty ratio changes, i.e., $f_{con} = 2kHz$. A second order discrete-time low pass Butterworth filter was applied to the collected data series, once forward and then reverse to eliminate any phase shift, see for example the `filtfilt` function in the MATLAB software environment. Then, the remaining steps were carried out, as outlined previously, under three different operating conditions of insolation and temperature. Specifically, in case 1 $S = 0.57\ kW/m^2$, $T = 23°C$, in case 2 $S = 0.45\ kW/m^2$, $T = 30°C$, and in case 3 $S = 0.61\ kW/m^2$, $T = 36°C$. The collected and filtered data, both I and V versus time, for the three cases are shown in Figure 7.

The results of the parameter identification steps are listed in Table 3. It can be seen from the results in the table that the relative errors are very low. Specifically, in all cases at the MPP they are less than 1.23% for V_m, 0.97% for I_m, and 1.61% for P_m. Moreover, the maximum error indices for the first and second identification models given in (13) and (22) were $EI_1 = 0.0053$ and $EI_2 = 0.2169$, respectively, showing

TABLE 3. Detailed validation results of the experiment.

		Case 1	Case 2	Case 3
S (kW/m^2)		0.57	0.45	0.61
Cell Temp. T_c (°C)		23	30	36
I_{ph} (A)	Estimated	1.6676	1.3298	1.7819
R_p (Ω)	Estimated	3.5511	4.088	3.0858
α (V)	Estimated	0.011709	0.014418	0.014442
I_0 (A)	Estimated	5.465×10^{-23}	6.849×10^{-18}	2.206×10^{-17}
P_m (W)	Actual	30.019	22.085	29.285
	Estimated	29.796	21.924	28.815
	Error (%)	0.74	0.73	1.61
V_m (V)	Actual	20.35	18.73	18.39
	Estimated	20.10	18.68	18.27
	Error (%)	1.23	0.26	0.64
I_m (A)	Actual	1.4751	1.1792	1.5927
	Estimated	1.4824	1.1737	1.5772
	Error (%)	0.50	0.47	0.97
EI_1		0.0050	0.0053	0.0035
EI_2		0.1989	0.1502	0.2169
$\bar{e}_I$ (%)		0.35	0.39	0.26
$\bar{e}_V$ (%)		0.74	0.83	1.43
Data Points N_{sc}		892	823	806
Total Data Points N			1000	
Data Collec. Time (s)			0.62	
Param. Ident. Time (s)			0.11	
Total Exec. Time (s)			0.73	
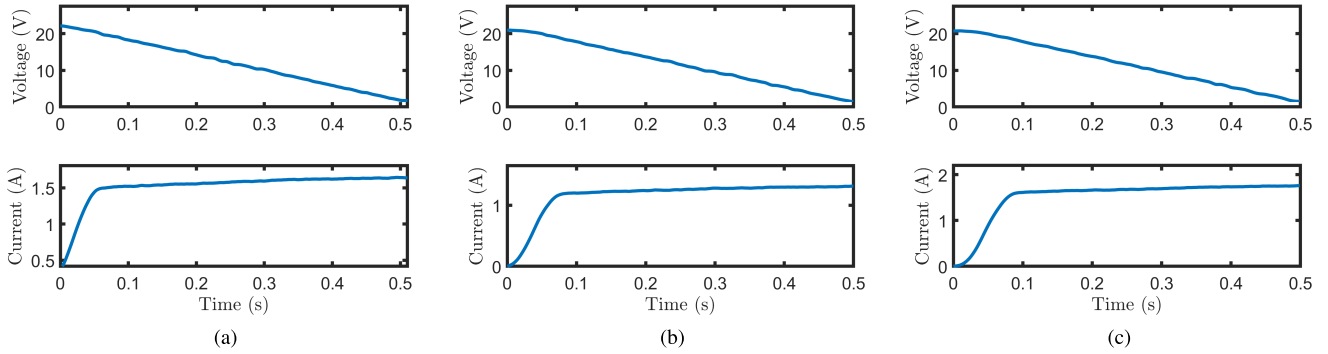
FIGURE 7. Experimental *V* and *I* vs. time for all three cases, (a) case 1, (b) case 2, and (c) case 3.
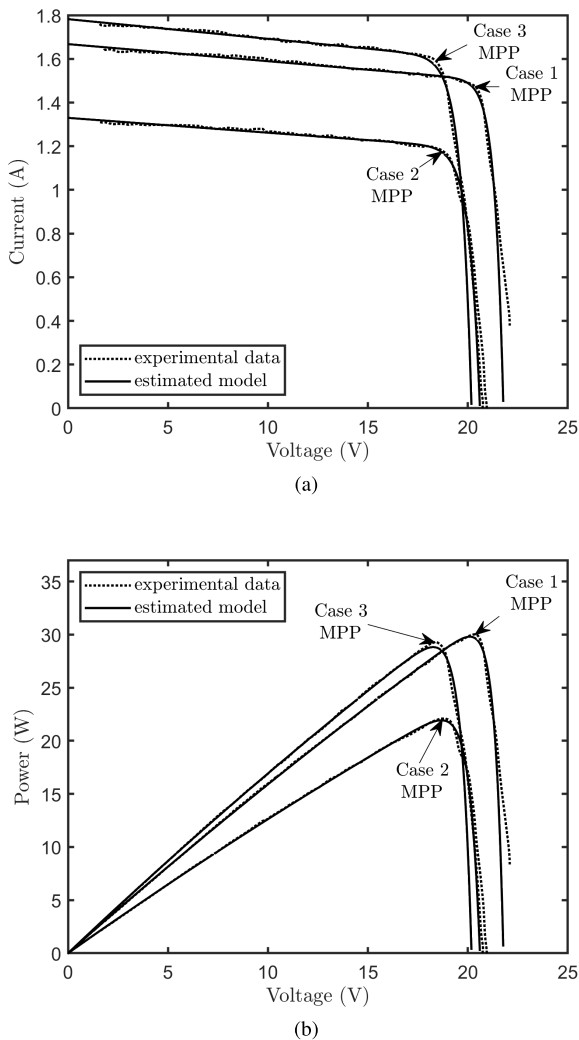
FIGURE 8. Experimental data vs. estimated model for all three cases, (a) *I-V* curves, and (b) *P-V* curves.

negligible discrepancy between the estimated model and the collected (and filtered) data in this region. On the other hand, the $\bar{e}_V$ reaches up to 1.43% (case 3) in the voltage-source region as a result of ignoring R_s in the SSDM.

Furthermore, the estimated *I-V* and *P-V* model curves for all three cases are plotted alongside the collected and filtered experimental data in Figures 8a and 8b, respectively. It can be seen that these curves are closely matched particularly in the current-source region, around the MPP, and well into the voltage-source region. This result is not obtainable in the current-source region if R_p is ignored. However, the impact of ignoring R_s in the SSDM equations is that there is a discernable discrepancy between the *I-V* curves of the measurements and estimated model in the voltage-source range near the V_{oc}, particularly in case 3. Therefore, the algorithm consistently yields a closely matched model for the collected experimental data under each one of these varied conditions.

A noteworthy remark is that the majority of data points obtained were in the current-source region in this DC Microgrid setup. In all three cases, N_{sc} is more than 800 data points, i.e., the number of points from I_{sc} down to $0.9I_{sc}$, see Table 3. This is despite evenly varying the duty ratio of the boost converter (in fixed increments) between 0 and 99% over $N = 1000$ points. Therefore, the current-source region can provide a wider practical range of operating points for the control of the PV DER's power output under these settings compared to the voltage-source region.

In all cases, the model was successfully identified online in under 1 second. In fact, it took only 0.11 seconds to perform the filtering and identification calculations on the Arm Cortex M3 microcontroller. This demonstrates the reliability and low computational complexity of implementing this algorithm online; which in turn facilitates frequently reapplying it in a PV DER system as conditions change throughout the day.

V. CONCLUSION

A non-iterative parameter identification method was developed in this work for PV modules and implemented on the restricted online operation scenario where they are connected to regulated DC Microgrids. The practical restrictions in the

that the parameters resulted in a very good fit to the data used in the estimation. In addition, the NRE in the current-source region $\bar{e}_I$ is less than 0.4% for all three cases, demonstrating a

time allowed for data collection and parameter identification, and the low complexity (in time and memory) required for it to be implemented online on the microcontroller of a PV DER system were addressed. Validation steps were undertaken in an experimental setup, where an accurate estimate of the *I-V* and *P-V* characteristic curves was achieved. Specifically, relative errors that are less than 1.6% where recorded in calculating P_m, and a total execution time of 0.73 seconds on an Arm Cortex M3 microcontroller was consistently achieved under different temperature and insolation conditions. Future work can focus on adopting the proposed method in DER controllers to accurately and quickly target specific power output levels in DC Microgrids. This would enhance DC Microgrids, encouraging their adoption as a reliable and efficient paradigm in smart grids. In addition, more work could focus on the development of a similar non-iterative method for the full SDM, i.e., with R_s, or higher order models.

REFERENCES

[1] D. E. Olivares, A. Mehrizi-Sani, A. H. Etemadi, C. A. Cañizares, R. Iravani, M. Kazerani, A. H. Hajimiragha, O. Gomis-Bellmunt, M. Saeedifard, R. Palma-Behnke, G. A. Jiménez-Estévez, and N. D. Hatziargyriou, "Trends in microgrid control," *IEEE Trans. Smart Grid*, vol. 5, no. 4, pp. 1905–1919, May 2014.

[2] T. Dragičević, X. Lu, J. C. Vasquez, and J. M. Guerrero, "DC microgrids—Part I: A review of control strategies and stabilization techniques," *IEEE Trans. Power Electron.*, vol. 31, no. 7, pp. 4876–4891, Jul. 2016.

[3] D. Chen and L. Xu, "AC and DC microgrid with distributed energy resources," in *Technologies and Applications for Smart Charging of Electric and Plug-in Hybrid Vehicles*. Cham, Switzerland: Springer, 2017, pp. 39–64.

[4] K. Kennerud, "Analysis of performance degradation in CdS solar cells," *IEEE Trans. Aerosp. Electron. Syst.*, vol. AES-5, no. 6, pp. 912–917, Nov. 1969.

[5] G. M. Masters, *Renewable and Efficient Electric Power Systems*. Hoboken, NJ, USA: Wiley, 2013.

[6] M. Haouari-Merbah, M. Belhamel, I. Tobías, and J. M. Ruiz, "Extraction and analysis of solar cell parameters from the illuminated current–voltage curve," *Sol. Energy Mater. Sol. Cells*, vol. 87, pp. 225–233, May 2005.

[7] M. Hejri, H. Mokhtari, M. R. Azizian, M. Ghandhari, and L. Soder, "On the parameter extraction of a five-parameter double-diode model of photovoltaic cells and modules," *IEEE J. Photovolt.*, vol. 4, no. 3, pp. 915–923, May 2014.

[8] K. Nishioka, N. Sakitani, Y. Uraoka, and T. Fuyuki, "Analysis of multicrystalline silicon solar cells by modified 3-diode equivalent circuit model taking leakage current through periphery into consideration," *Sol. Energy Mater. Sol. Cells*, vol. 91, no. 13, pp. 1222–1227, Aug. 2007.

[9] J. C. H. Phang, D. S. H. Chan, and J. R. Phillips, "Accurate analytical method for the extraction of solar cell model parameters," *Electron. Lett.*, vol. 20, no. 10, pp. 406–408, May 1984.

[10] F. J. Toledo, J. M. Blanes, and V. Galiano, "Two-step linear least-squares method for photovoltaic single-diode model parameters extraction," *IEEE Trans. Ind. Electron.*, vol. 65, no. 8, pp. 6301–6308, Aug. 2018.

[11] E. Moshksar and T. Ghanbari, "Adaptive estimation approach for parameter identification of photovoltaic modules," *IEEE J. Photovolt.*, vol. 7, no. 2, pp. 614–623, Mar. 2017.

[12] L. H. I. Lim, Z. Ye, J. Ye, D. Yang, and H. Du, "A linear identification of diode models from single $I − V$ characteristics of PV panels," *IEEE Trans. Ind. Electron.*, vol. 62, no. 7, pp. 4181–4193, Jul. 2015.

[13] D. Sera, R. Teodorescu, and P. Rodriguez, "PV panel model based on datasheet values," in *Proc. IEEE Int. Symp. Ind. Electron. (ISIE)*, Jun. 2007, pp. 2392–2396.

[14] M. G. Villalva, J. R. Gazoli, and E. R. Filho, "Comprehensive approach to modeling and simulation of photovoltaic arrays," *IEEE Trans. Power Electron.*, vol. 24, no. 5, pp. 1198–1208, May 2009.

[15] E. Saloux, A. Teyssedou, and M. Sorin, "Explicit model of photovoltaic panels to determine voltages and currents at the maximum power point," *Sol. Energy*, vol. 85, no. 5, pp. 713–722, May 2011.

[16] W. Xiao, M. G. J. Lind, W. G. Dunford, and A. Capel, "Real-time identification of optimal operating points in photovoltaic power systems," *IEEE Trans. Ind. Electron.*, vol. 53, no. 4, pp. 1017–1026, Jun. 2006.

[17] H. Andrei, T. Ivanovici, G. Predusca, E. Diaconu, and P. C. Andrei, "Curve fitting method for modeling and analysis of photovoltaic cells characteristics," in *Proc. IEEE Int. Conf. Automat., Quality Test., Robot. (AQTR)*, May 2012, pp. 307–312.

[18] B. Paviet-Salomon, J. Levrat, V. Fakhfouri, Y. Pelet, N. Rebeaud, M. Despeisse, and C. Ballif, "Accurate determination of photovoltaic cell and module peak power from their current–voltage characteristics," *IEEE J. Photovolt.*, vol. 6, no. 6, pp. 1564–1575, Nov. 2016.

[19] H. Ibrahim and N. Anani, "Evaluation of analytical methods for parameter extraction of PV modules," *Energy Proc.*, vol. 134, pp. 69–78, Oct. 2017.

[20] M. Zagrouba, A. Sellami, M. Bouaïcha, and M. Ksouri, "Identification of PV solar cells and modules parameters using the genetic algorithms: Application to maximum power extraction," *Sol. Energy*, vol. 84, no. 5, pp. 860–866, 2010.

[21] M. Azab, "Identification of one-diode model parameters of PV devices from nameplate information using particle swarm and least square methods," in *Proc. 1st Workshop Smart Grid Renew. Energy (SGRE)*, Mar. 2015, pp. 1–6.

[22] H. Qin and J. W. Kimball, "Parameter determination of photovoltaic cells from field testing data using particle swarm optimization," in *Proc. IEEE Power Energy Conf. Illinois*, Feb. 2011, pp. 1–4.

[23] F. Bradaschia, M. C. Cavalcanti, A. J. do Nascimento, E. A. da Silva, and G. M. de Souza Azevedo, "Parameter identification for PV modules based on an environment-dependent double-diode model," *IEEE J. Photovolt.*, vol. 9, no. 5, pp. 1388–1397, Sep. 2019.

[24] H. G. G. Nunes, P. N. C. Silva, J. A. N. Pombo, S. J. P. S. Mariano, and M. R. A. Calado, "Multiswarm spiral leader particle swarm optimisation algorithm for PV parameter identification," *Energy Convers. Manage.*, vol. 225, Dec. 2020, Art. no. 113388.

[25] M.-U.-N. Khursheed, M. A. Alghamdi, M. F. N. Khan, A. K. Khan, I. Khan, A. Ahmed, A. T. Kiani, and M. A. Khan, "PV model parameter estimation using modified FPA with dynamic switch probability and step size function," *IEEE Access*, vol. 9, pp. 42027–42044, 2021.

[26] A. Sharma, A. Sharma, A. Dasgotra, V. Jately, M. Ram, S. Rajput, M. Averbukh, and B. Azzopardi, "Opposition-based tunicate swarm algorithm for parameter optimization of solar cells," *IEEE Access*, vol. 9, pp. 125590–125602, 2021.

[27] M. Premkumar, P. Jangir, C. Ramakrishnan, G. Nalinipriya, H. H. Alhelou, and B. S. Kumar, "Identification of solar photovoltaic model parameters using an improved gradient-based optimization algorithm with chaotic drifts," *IEEE Access*, vol. 9, pp. 62347–62379, 2021.

[28] L. Li, G. Xiong, X. Yuan, J. Zhang, and J. Chen, "Parameter extraction of photovoltaic models using a dynamic self-adaptive and mutual-comparison teaching-learning-based optimization," *IEEE Access*, vol. 9, pp. 52425–52441, 2021.

[29] T. Huang, C. Zhang, H. Ouyang, G. Luo, S. Li, and D. Zou, "Parameter identification for photovoltaic models using an improved learning search algorithm," *IEEE Access*, vol. 8, pp. 116292–116309, 2020.

[30] K. Lappalainen, P. Manganiello, M. Piliougine, G. Spagnuolo, and S. Valkealahti, "Virtual sensing of photovoltaic module operating parameters," *IEEE J. Photovolt.*, vol. 10, no. 3, pp. 852–862, May 2020.

[31] T. Stewart. (2021). Basic linear algebra library. GitHub. [Online]. Available: https://github.com/tomstewart89/BasicLinearAlgebra

[32] A. M. A. Oteafy, J. N. Chiasson, and S. Ahmed-Zaid, "Development and application of a standstill parameter identification technique for the synchronous generator," *Int. J. Electr. Power Energy Syst.*, vol. 81, pp. 222–231, Oct. 2016.

[33] A. M. A. Oteafy, "Fast and comprehensive online parameter identification of switched reluctance machines," *IEEE Access*, vol. 9, pp. 46985–46996, 2021.

[34] J. Chiasson, *Modeling and High Performance Control of Electric Machines*, vol. 26. Hoboken, NJ, USA: Wiley, 2005.

[35] Y. Chen, Y. Yao, and Y. Zhang, "A robust state estimation method based on SOCP for integrated electricity-heat system," *IEEE Trans. Smart Grid*, vol. 12, no. 1, pp. 810–820, Jan. 2021.

[36] G. Grandi, A. Ienina, and M. Bardhi, "Effective low-cost hybrid LED-halogen solar simulator," *IEEE Trans. Ind. Appl.*, vol. 50, no. 5, pp. 3055–3064, Sep./Oct. 2014.

AHMED M. A. OTEAFY (Senior Member, IEEE) received the B.S. and M.S. degrees in electrical engineering from Kuwait University, and the Ph.D. degree in electrical and computer engineering from Boise State University, ID, USA, in 2011. He is currently an Assistant Professor with Alfaisal University, Riyadh, Saudi Arabia, and the Director of the Joint Smart Grids and Electric Vehicles Research and Development Center (JSEC). His research interests include smart power grids and electric machines, such as modeling, parameter identification, control, and design of cyber physical power systems, generators and motors, specifically, large synchronous generators, induction motors, switched reluctance machines, battery-energy storage systems, and DC microgrids. He is also developing Research and Development testbeds for DC microgrids, active battery pack balancing, and a boeing-funded solar car project.

ARAM S. MONAWAR (Member, IEEE) received the bachelor's degree (Hons.) in electrical engineering from Alfaisal University, in 2018, and the M.S. degree in electrical and computer engineering from the Georgia Institute of Technology, Atlanta, Georgia, USA, in 2020. Her technical focus was in the area of systems and control. She was a Research Assistant with the Joint Smart Grids and Electric Vehicles Research and Development Center (JSEC) for two years. She is currently an Instructor of electrical engineering with Alfaisal University. In addition to the experience of working with the DC microgrid cyber-physical energy systems, she was a five year Senior Member of the Alfaisal Solar Car Project.

• • •

ABDULRAHMAN ABOMAZID (Member, IEEE) was born in Riyadh, Saudi Arabia, in 1995. He received the Bachelor of Engineering (B.Eng.) degree in the field of electrical engineering from Alfaisal University, Riyadh, in 2018, and the M.A.Sc. degree in electrical engineering and computer science from the Lassonde School of Engineering, York University, Ontario, Canada, in 2021. He joined as a Research Assistant with the Joint Smart Grids and Electric Vehicles Research & Development Center (JSEC), Alfaisal University, in 2018, and as of 2019 remains as an Affiliate Member. Since September 2019, he has been working as a Research Assistant and a Teacher Assistant with the Department of Electrical Engineering and Computer Science (EECS), York University. His current research interests include energy conversion, microgrids, and renewable energy systems integration.